

Supplemental Theory S1:

Corrections to diffusion coefficient in the endogenous radial diffusion model of Wang et al. (2015)

As discussed in Wang et al. (2015), bubble pressure in recently cavitating vessels can grow to a sub-atmospheric pressure in very short time from endogenous air in a kind of quasi-equilibrium by gas diffusion from a cylindrical annulus about 50 μm in radius. The endogenous source of air is (1) the water in the cavitating vessels before cavitation events happen and (2) the capillary water in stem that is not pulled out, which is held on non-cavitating vessels and water in fibers and living cells. However, the endogenous air from the tissue water adjacent to the vessel is not enough for the bubble pressure to reach ambient barometric pressure. Air dissolved in the vessel water and surrounding tissues would be drawn into the cavitating vessels very fast by diffusion over short distances. Hence the vessels have to accumulate air from exogenous sources from beyond the bark and/or from air dissolved in flowing water in the nearby conductive vessels to build up the ultimate equilibrium bubble pressure. Experimental results show that the mean half time for bubble pressurization is 17 to 18 h. The air sources and air transport processes are described in more detail below.

When vessels cavitate, the air dissolved in water (source 1 and 2) will be drawn out very fast together with water vapor and these gases will fill the vessel lumen as shown in Fig. S1. Fig. S1 differs from Fig. S2 in Wang et al. (2015) because the diffusion coefficient used in this paper is a measured value in wet wood ($D = 1.0\text{E-}6 \text{ cm}^2 \text{ s}^{-1}$), while Wang et al. (2015) used the value for pure water $D = 2.0\text{E-}5 \text{ cm}^2 \text{ s}^{-1}$ (Soriz and Hietz, 2005). Hence Wang et al. (2015) erroneously estimated the time of localized radial diffusion as being equal to 5 s; but after re-computation using the measured D the localized equilibration is still fast (less than 2 min). However, both of the two endogenous sources contribute only to the initial bubble pressure in < 2 minutes; this endogenous diffusion process continues until a localized equilibrium is reached as determined by Eq. (1) in Wang et al. (2015).

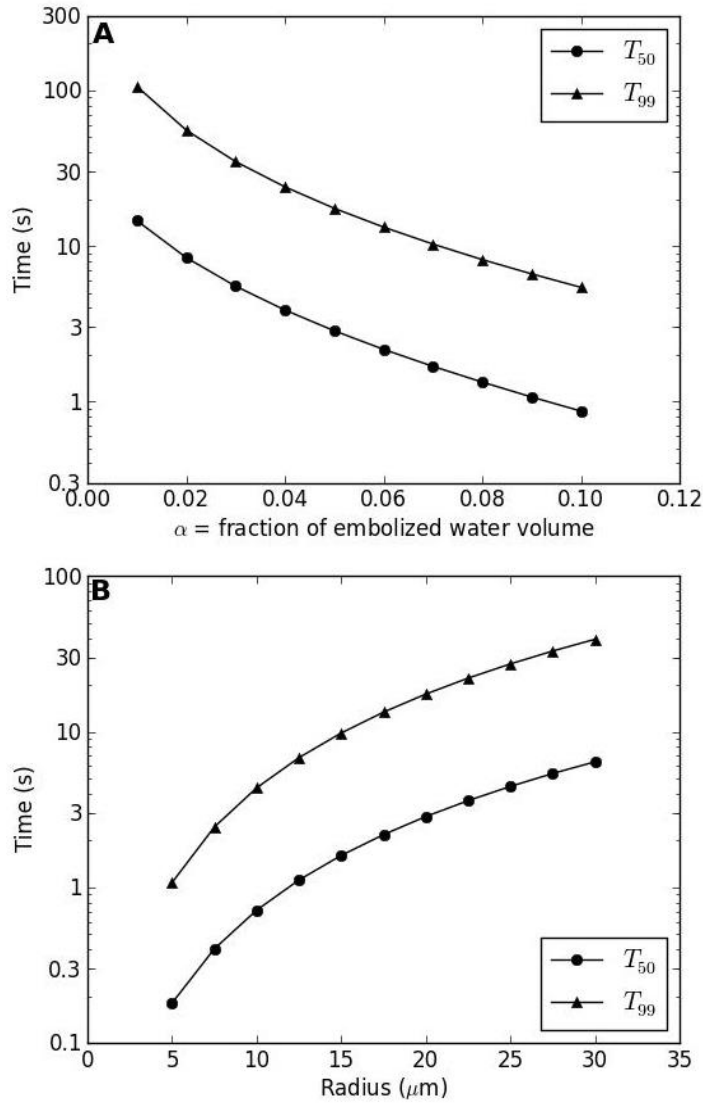


Figure S1. Relationship between α /radius and the half time and 99% equilibrium time. T_{50} and T_{99} refer to the half time (solid circle) and 99% equilibrium time (solid triangle), respectively. Panel A: half time and 99% equilibrium time of the vessel with radius of 20 μm when α range from 0.01 to 0.10. And in panel A α represents the fraction of embolized water volume in the stem. Panel B: half time and 99% equilibrium time of the vessel with diameter range from 5 to 30 μm when α is 0.05.

Supplemental Appendix S1: Exogenous source: model of radial diffusion through the wood

Fick's law governs the diffusion of dissolved air through liquid, and the concentration of dissolved air at the air/water interface can be computed by Henry's law (details in supplemental materials of Wang et al. (2015)). The rate of air diffusion through the stem can be computed by dividing the stem into a finite number of thin shells.

Treating the stem as a cylinder with external xylem radius R_{out} and internal radius $R_{in} = 0$; the xylem is divided into N shells with thickness of $\Delta x = (R_{out} - R_{in})/N$ for each shell. The boundaries of the N shells are $[R_{out}, R_{out} - \Delta x, \dots, R_{out} - i \cdot \Delta x, \dots, R_{in} + \Delta x, R_{in}]$. It is worth noting that the last 'shell' in the center is a cylinder with no internal boundary. Also the central

cylinder and maybe some adjacent shells could be pith, but less is known of property of the pith, therefore we treat it like wood. The geometrical center of i th shell is $x_i = \sqrt{(R_i^2 + R_{i+1}^2)}/2$, where R_i and R_{i+1} are the radius of outer and inner boundary respectively and the volume of i th shell of length L is $V_i = \pi \cdot ((R_i^2 - R_{i+1}^2)) \cdot L$. The cylindrical diffusion equations (Eq. A1.7a and Eq. A1.7b) in the appendix of Wang et al. (2015) is adopted to compute the concentration changes in each shell. It is worth noting that the diffusion coefficient of O_2 measured in wet wood is much lower than that of pure water, therefore the diffusion coefficient of air in wet wood $D = 1.0E-6 \text{ cm}^2 \text{ s}^{-1}$ is used (Soraz and Hietz, 2005), which is about 0.05 of that of in pure water. Since wood consists of a meshwork of cell walls with water-filled lumina (vessel and fiber lumina), we can imagine that the diffusion coefficient of the wall component must be much less than 10^{-6} because the water-filled lumina have D values of $2 \times 10^{-5} \text{ cm}^2 \text{ s}^{-1}$. The value of D in the lignified walls must be much lower than $1E-6$ because the measured value ($1E-6$) is the blended average for the complex wood structure. The measured diffusion coefficient is also anisotropic, more axially than radially, but we can ignore the axial component since we can rely on axial symmetry in our radial diffusion calculations.

In a time interval of Δt , the moles of gas diffuse through two adjacent shells can be computed by

$$\Delta n_i = 2\pi D_A \cdot \frac{C_{A,i-1} - C_{A,i}}{\ln(x_{i-1}/x_i)} \cdot L \cdot \Delta t \quad (\text{A2.1})$$

, where $C_{A,i}$ is the concentration of air in the i th shell and $C_{A,0}$ is the equilibrated gas concentration at the external water/air interface, D_A is the diffusion coefficient of air. The outer surface of the outer shell has $x_0 = R_{\text{out}}$; hence the diffusion distance is half the normal distance between shells. Because of the fast localized equilibrium between bubbles and surrounding tissue, Henry's law must be called into use to compute how much air that diffused into one shell actually stays in the water versus the amount that migrates to the bubble.

The localized equilibrium can be computed from Henry's law, which basically predicts that the increase of concentration of air in water is a fraction, f_w , of the air entering the cylindrical annulus. The localized equilibrium (assuming fast localized diffusion) can be computed from the volume fraction that is bubble, α , and applying mass conservation between moles of gas entering a cylindrical shell and the division of that mass between water and air during the localized equilibration. The derivation of the fraction, f_w , that stays in the water (not shown) yields:

$$f_w = \frac{n_w}{n_w + n_b} = \frac{(1 - \alpha) \cdot K_A}{(1 - \alpha) \cdot K_A + \alpha/RT} \quad (\text{A2.2})$$

69 where n_w and n_b is the moles of air that stays in water and bubble respectively. Hence the
70 concentration change of each shells and the bubble pressure in the bubble can be computed by:

$$\Delta C_{A,i} = \frac{\Delta n_{i-1} - \Delta n_i}{(1 - \alpha)V_i} \cdot f_w \quad (\text{A2.3a})$$

$$\Delta P_i = \Delta C_{A,i}/K_A \quad (\text{A2.3b})$$

71 On iterating through all the shells after a given time interval, the concentration or bubble
72 pressure in each shells can be evaluated from Eq. A2.3b.

73 The volume weighted averaged bubble pressure was computed from the sum of the shells:
74 $\bar{P}_b = \sum(P_i \cdot V_i) / \sum V_i = \sum(K_A \cdot C_i \cdot V_i) / \sum V_i$, where P_i and C_i are the bubble pressure and air
75 concentration in i th shell, V_i is the shell volume, and K_A is the Henry's law constant of air. The
76 volume averaged bubble pressure is arguably what was computed by the methods in Wang et
77 al. (2015) so model results were computed on the same basis. The equations above were used
78 to calculate the values shown in Fig. 8.

79

80 **Supplemental Appendix S2: Exogenous source: catena of embolized vessels**

81 An alternative way of looking at gas transfer into the embolized vessels is that gas exchange
82 through two adjacent embolized vessels via diffusion through the pit membranes in common
83 between them. It could be argued that the diffusion coefficient of air through un-lignified pit
84 membranes might be higher than through the lignified walls, but a model of catena flow from
85 vessel to vessel via pits is uncertain for several reasons: (1) the value of D for pits is unknown,
86 (2) the pit area in common between two adjacent, embolized vessels is unknown for our species
87 but known for related species, (3) how much of the diffusion goes between vessel through
88 lignified cell walls of vessels and fibers when the vessel are not in contact cannot be
89 independently evaluated, and (4) the geometry of the catena (how it passing through the 3D
90 structure of the wood) is also unknown. The lack of 3D knowledge of the catena makes it
91 impossible to relate computed pressure changes in a catena to the volume averaged bubble
92 pressure in the wood, which we argue is what is measured. Nevertheless some qualitative
93 insights into the gas transfer through a catena of vessels can be gained by doing some
94 calculations even though we cannot say if the catena diffusion process is a major contributor
95 to the overall transport processes in the wood.

Assume that all the vessels have similar geometry, vessel length of L_v , vessel diameter of D_v , contact fraction of f_c (area fraction of the vessel that is contacted with other vessels), and pit field fraction of f_p (area fraction of the contact area that is pit). Then the total area for diffusion between two vessels is

$$S_p = \pi \cdot D_v \cdot L_v \cdot f_c \cdot f_p \quad (\text{A3.1})$$

, and the moles transferred by diffusion through the pits of thickness L_p in a given Δt is

$$J_{out,in} = D \cdot S_p / N_c \cdot \frac{C_{out} - C_{in}}{L_p} \cdot \Delta t = D \cdot S_p \cdot K_A \cdot \frac{P_{out} - P_{in}}{L_p} \cdot \Delta t \quad (\text{A3.2})$$

, where $J_{out,in}$ is the moles transferred from source vessel to the sink vessel, N_c is the number of vessels that contact with the target vessel. In this calculation we treat the simplest example of a linear (unbranched) catina. In a catina diffusional pathway, the moles change in the i th vessel should be the sum of input from the $(i-1)$ th and output to the $(i+1)$ th vessel, that is

$$IO_i = J_{i-1,i} - J_{i,i+1} \quad (\text{A3.3})$$

, and the bubble pressure change in the i th vessel can be computed by

$$\Delta P_i = \frac{IO_i}{V_v} \cdot RT \quad (\text{A3.4})$$

, where V_v is the volume of the vessel. As in the radial diffusion model, Henry's law should be called to compute the final pressure change, namely $\Delta P_{i,e} = f_b \cdot \Delta P_i$, where $f_b = 1 - f_w$ is the fraction of air that stays in the bubble.

Eq. A3.2 reveals that the diffusion rate between two adjacent cavitated vessels is correlated to the pressure difference, so we can infer that the pressure change caused by the diffusion can be simply computed by $dP = k \cdot \Delta P$.

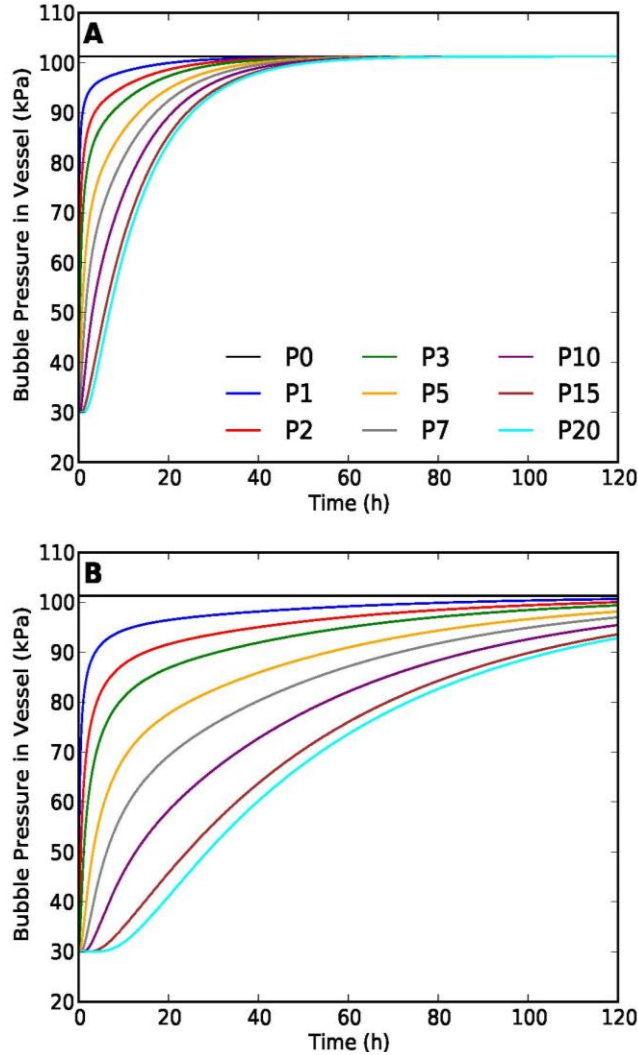


Figure S2. This plot shows theoretical bubble pressure changes in 20 consecutive cavitated vessels in two species. P_N is the bubble pressure in the N th vessel. Panel A shows the trend of bubble pressures change in *Acer mono* and panel B shows that of *Populus 84K*. The coefficient constants between two adjacent embolized vessels used were 0.101 and $0.024 \text{ kPa}^{-1} \text{ s}^{-1}$ for *Acer mono* and *Populus 84K* respectively, and the time interval Δt used was 1 s .

The parameters we used here for *Acer mono* ($A.$) and *Populus 84K* ($P.$) are: vessel lengths are 2.877 ($A.$) and 7.165 ($P.$) cm; the vessel diameters are 26.1 ($A.$) and 32.5 ($P.$) μm ; the contact fractions are 0.30 ($A.$) and 0.11 ($P.$); the pit field fractions are 0.69 ($A.$) and 0.49 ($P.$); the thickness of bordered pit is $1 \mu\text{m}$ for both species. The contact fraction and pit field fraction of $A.$ are from the same genus species while those of $P.$ are from the average of a variety of species (Hacke et al., 2006). The k values of $A.$ and $P.$ are $5.27\text{E-}3$ and $1.26\text{E-}3 \text{ s}^{-1}$, respectively.

The bubble pressure change in a catena of 20 vessels is plotted in Fig. S2 and the half times of the 20 vessels are plotted in Fig S3. The back-to-envelop computation also showed slow bubble pressurization when $N > 20$, but less knowledge is known to make the prediction accurate.

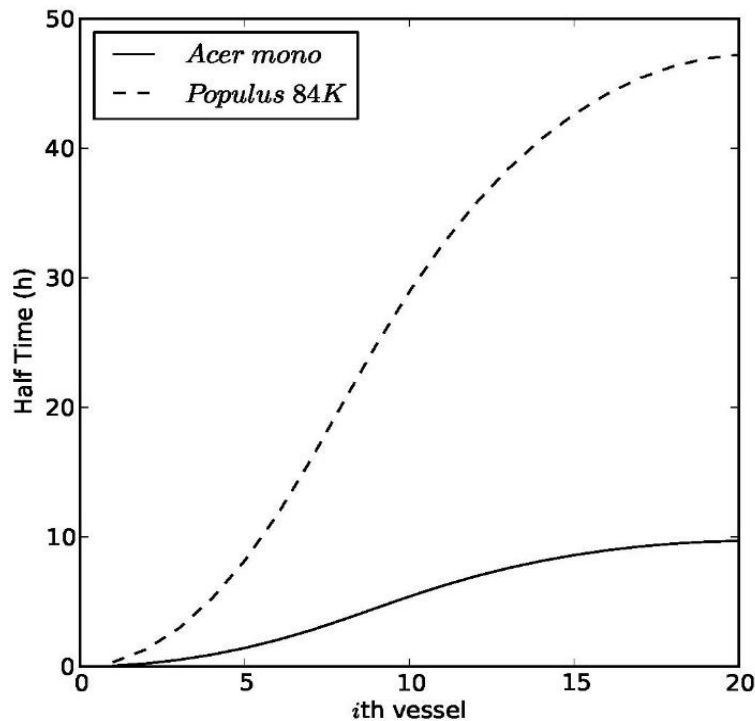


Figure S3. Half time of the i th vessel in a catena of vessels. The initial bubble pressure of embolized vessels is 30 kPa and the atmospheric pressure is 101.3 kPa. Half time in each vessel is the time spent to increase the bubble pressure to 65.65 kPa.

In conclusion, the catena model provides some new insights into some of the processes involved in radial diffusion thru wood consisting of a mixture of solids, water and air bubbles. However, the model results solves for only part of the processes, i.e., pathways of diffusion. The entire process is more precisely modeled by Appendix S2 because it uses a bulk diffusion coefficient measured in wood and the diffusional processes involved in the experimentally measurement of D found in Sorz and Hietz (2005) would already include the contribution of the catena processes calculated above as well as other diffusional mechanisms (or pathways). Hence we think the catena model has little predictive value for the overall transport processes measured in this paper and in Wang et al. (2015) but the model does provide some interesting qualitative information about one contributing pathway.

Literature Cited

- 135 **Hacke UG, Sperry JS, Wheeler JK, Castro L** (2006) Scaling of angiosperm xylem structure
136 with safety and efficiency. *Tree Physiol* **26**: 689-701
- 137 **Sorz J, Hietz P** (2005) Gas diffusion through wood: implications for oxygen supply. *Trees* **20**:
138 34-41
- 139 **Wang Y, Pan R, Tyree MT** (2015) Studies on the tempo of bubble formation in recently
140 cavitated vessels: A model to predict the pressure of air bubbles. *Plant Physiol*